

Anomalous large conductance fluctuations in weakly disordered graphene

A. Rycerz,¹ J. Tworzydło,² and C. W. J. Beenakker³

¹*Marian Smoluchowski Institute of Physics, Jagiellonian University, Reymonta 4, 30-059 Kraków, Poland*

²*Institute of Theoretical Physics, Warsaw University, Hoża 69, 00-681 Warsaw, Poland*

³*Instituut-Lorentz, Universiteit Leiden, P.O. Box 9506, 2300 RA Leiden, The Netherlands*

(Dated: December 2006)

We have studied numerically the mesoscopic fluctuations of the conductance of a graphene strip (width W larger than length L), in an ensemble of samples with different realizations of the random electrostatic potential landscape. For strong disorder (potential fluctuations comparable to the hopping energy), the variance of the conductance approximates the value predicted by the Altshuler-Lee-Stone theory of universal conductance fluctuations, $\text{Var } G_{\text{UCF}} = 0.12 (W/L)(2e^2/h)^2$. For weaker disorder the variance is greatly enhanced if the potential is smooth on the scale of the atomic separation. There is no enhancement if the potential varies on the atomic scale, indicating that the absence of backscattering on the honeycomb lattice is at the origin of the anomalously large fluctuations.

PACS numbers: 73.23.-b, 72.15.Rn, 73.40.-c, 73.63.Nm

Phase coherent diffusion in metals is accompanied by sample-to-sample fluctuations in the conductance of the order of the conductance quantum e^2/h , dependent on the shape of the conductor but independent of its size or of the disorder strength. This is the phenomenon of universal conductance fluctuations (UCF) [1, 2]. The universality does not extend to different transport regimes, in particular the fluctuations become much *smaller* than the UCF value both in the ballistic regime of weak disorder and in the localized regime of strong disorder [3, 4].

In this paper we report on the observation in a computer simulation of a transport regime with conductance fluctuations that are much *larger* than the UCF value. The anomalously large fluctuations appear in a tight-binding model of a carbon monolayer, for a disorder potential that is smooth on the scale of the atomic separation and weak on the scale of the hopping energy. It is known that such a potential in a honeycomb lattice can deflect the electrons but cannot scatter them backwards [5, 6]. The consequences for weak localization of the absence of backscattering have been studied theoretically [7, 8, 9, 10] and experimentally [11, 12]. While conductance fluctuations as a function of magnetic field in a given sample have been observed experimentally [11, 13, 14], and analyzed in terms of the UCF theory, the anomaly found here in the sample-to-sample fluctuations has not been reported previously.

We consider a disordered strip of graphene in the $x-y$ plane, connected to ballistic leads at $x = 0$ and $x = L$ (see Fig. 1). The orientation of the honeycomb lattice is such that the edges at $y = 0$ and $y = W$ are in the zigzag configuration. We vary L and W at fixed aspect ratio (mostly taking a rather large ratio $W/L = 3.03$ to minimize the effects of edge states). The lattice Hamiltonian is

$$H = \sum_{i,j} \tau_{ij} |i\rangle \langle j| + \sum_i [U_{\text{gate}}(\mathbf{r}_i) + U_{\text{imp}}(\mathbf{r}_i)] |i\rangle \langle i|. \quad (1)$$

The hopping matrix element $\tau_{ij} = -\tau$ if the orbitals

$|i\rangle$ and $|j\rangle$ are nearest neighbors (with $\tau \approx 3\text{ eV}$), otherwise $\tau_{ij} = 0$. The velocity v near the Dirac point equals $v = \frac{1}{2}\sqrt{3}\tau a/\hbar \approx 10^6\text{ m/s}$, with $a = 0.246\text{ nm}$ the lattice constant.

The electrostatic potential contains a contribution U_{gate} from gate electrodes and a random contribution U_{imp} from impurities. The potential U_{gate} vanishes in the leads $x < 0$ and $x > L$ and equals U_0 in the strip $0 < x < L$. By varying U_0 at fixed Fermi energy μ_∞ in the leads, we can vary the Fermi energy $\mu_0 = \mu_\infty - U_0$ in the strip. We take $\mu_\infty = \tau/2$ and compare the two cases $U_0 = \mu_\infty \Rightarrow \mu_0 = 0$ and $U_0 = 0 \Rightarrow \mu_0 = \mu_\infty$. The first case is an undoped graphene strip, the second case is a heavily doped strip (but still at sufficiently small Fermi energy that the linearity of the dispersion relation holds reasonably well).

We generate a realization of the disorder potential by randomly choosing N_{imp} lattice sites $\mathbf{R}_1, \mathbf{R}_2, \dots, \mathbf{R}_{N_{\text{imp}}}$ out of the total number $N_{\text{tot}} = \frac{4}{3}\sqrt{3}LW/a^2$ of sites in the disordered strip, and by randomly choosing the potential amplitude U_n at the n -th site in the interval $(-\delta, \delta)$. We then smooth the potential over a range ξ by convolution with a Gaussian,

$$U_{\text{imp}}(\mathbf{r}) = \sum_{n=1}^{N_{\text{imp}}} U_n \exp\left(-\frac{|\mathbf{r} - \mathbf{R}_n|^2}{2\xi^2}\right). \quad (2)$$

In the special case $\xi \ll a$, $N_{\text{imp}} = N_{\text{tot}}$ each of the lattice sites in the strip has a randomly fluctuating potential. This is the Anderson model on a honeycomb lattice studied in Ref. [15]. We contrast this model of atomic-scale defects with the case $\xi = a\sqrt{3}$ of a potential which is still short-ranged on the scale of the system size but which varies smoothly on the atomic scale. Such a potential could be realized by screened charges in the substrate. (The Gaussian smoothing is chosen for computational convenience, and we have checked that the results are not sensitive to the type of smoothing considered.)

We quantify the disorder strength by the dimensionless

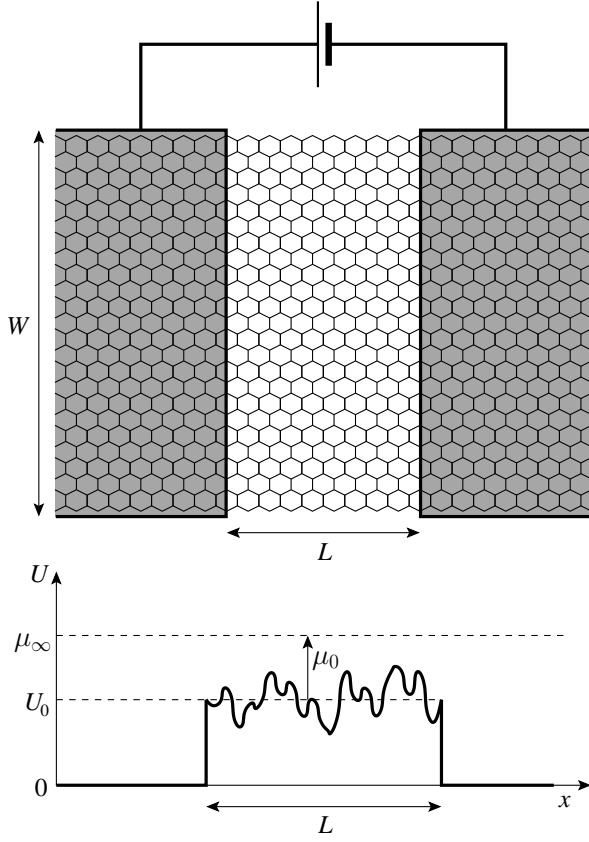


FIG. 1: Top panel: Top view of the honeycomb lattice in a graphene strip, connecting two electrical contacts at a voltage difference (gray rectangles). The samples used in the simulation are much larger than the one shown here. Bottom panel: Potential profile along the strip, showing the fluctuations from the disorder.

correlator

$$K_0 = \frac{LW}{(\hbar v)^2} \frac{1}{N_{\text{tot}}^2} \sum_{i=1}^{N_{\text{tot}}} \sum_{j=1}^{N_{\text{tot}}} \langle U_{\text{imp}}(\mathbf{r}_i) U_{\text{imp}}(\mathbf{r}_j) \rangle \quad (3)$$

of the random impurity potential (with vanishing average, $\langle U_{\text{imp}} \rangle = 0$). This single number K_0 is representative on length scales large compared to the correlation length ξ . For the model potential (2) we find (for $\xi \ll L, W$)

$$K_0 = \frac{1}{9} \sqrt{3} (\delta/\tau)^2 (N_{\text{imp}}/N_{\text{tot}}) \kappa^2, \quad (4)$$

$$\begin{aligned} \kappa &= \frac{1}{N_{\text{imp}}} \sum_{n=1}^{N_{\text{imp}}} \sum_{i=1}^{N_{\text{tot}}} \exp \left(-\frac{|\mathbf{r}_i - \mathbf{R}_n|^2}{2\xi^2} \right) \\ &= \begin{cases} 1 & \text{if } \xi \ll a, \\ \frac{8}{3} \pi \sqrt{3} (\xi/a)^2 & \text{if } \xi \gg a. \end{cases} \end{aligned} \quad (5)$$

For large μ_0 the correlator K_0 determines the transport mean free path l_{tr} in Born approximation [6, 7],

$$l_{\text{tr}} = \frac{2}{k_F K_0} \times \begin{cases} 2 & \text{if } \xi \gtrsim a, \\ 1 & \text{if } \xi \ll a, \end{cases} \quad (6)$$

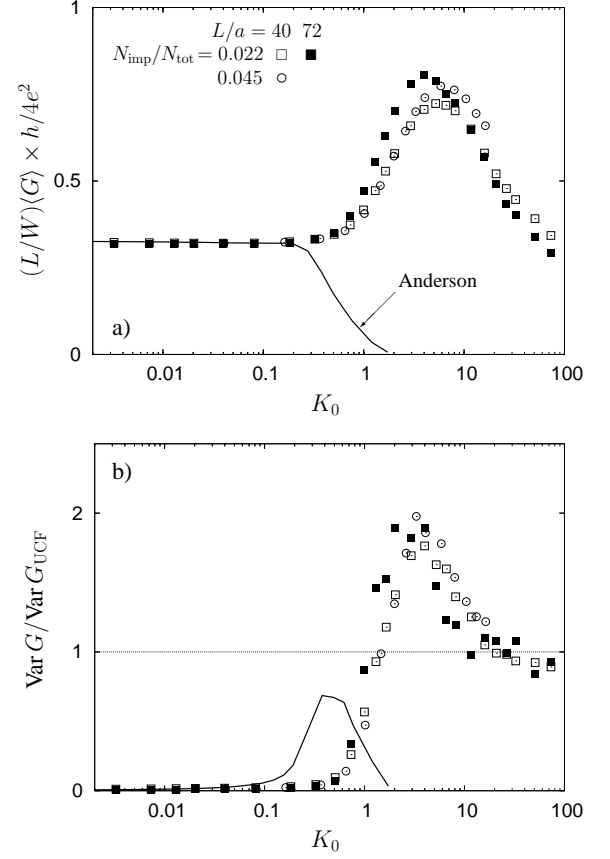


FIG. 2: Average and variance of the conductance as a function of the strength of the disorder potential, quantified by the correlator (3). These plots are for the case that the disordered strip is at the Dirac point ($\mu_0 = 0$). The data points are for a smooth, short-range impurity potential (correlation length $\xi = a\sqrt{3}$), with different values of the impurity density $N_{\text{imp}}/N_{\text{tot}}$. Open symbols are for $L = 40a$, filled symbols for $L = 72a$ (at fixed aspect ratio $W/L = 3.03$). The solid line is the Anderson model of atomic scale disorder ($\xi = 0$, $N_{\text{imp}} = N_{\text{tot}}$, $L = 40a$).

where $k_F = |\mu_0|/\hbar v$ is the Fermi wave vector in the strip (which should be $\gg 1/l_{\text{tr}}$ for the Born approximation to hold). The factor-of-two increase in l_{tr} for smooth disorder is due to the absence of backscattering in the honeycomb lattice [5, 6]. The corresponding “classical” conductivity (without quantum corrections) is given by $\sigma_{\text{class}} = (2e^2/h)k_F l_{\text{tr}}$.

We calculate the transmission matrix \mathbf{t} numerically by means of a recursive Green function algorithm. The conductance G then follows from the Landauer formula $G = (2e^2/h) \text{Tr } \mathbf{t} \mathbf{t}^\dagger$. (The factor of two accounts for the spin degeneracy.) By repeating the calculation for some 300–3000 realizations of the disorder potential, we obtain the average conductance $\langle G \rangle$ and the variance $\text{Var } G = \langle G^2 \rangle - \langle G \rangle^2$. Results are shown in Fig. 2 at the Dirac point ($\mu_0 = 0$) and in Fig. 3 at $\mu_0 = \tau/2$.

The Altshuler-Lee-Stone theory of universal conduc-

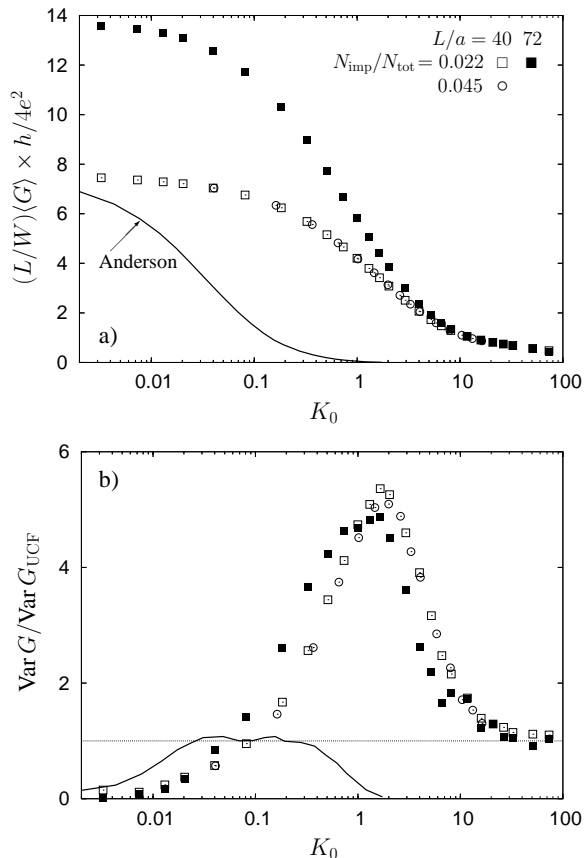


FIG. 3: Same as Fig. 2, but now for the case that the disordered strip is away from the Dirac point ($\mu_0 = \tau/2 = \mu_\infty$).

tance fluctuations (UCF) gives a variance [1, 2, 4]

$$\text{Var } G_{\text{UCF}} = C \frac{1}{\beta} \left(\frac{se^2}{h} \right)^2 \frac{W}{L}, \quad \text{if } W \gg L, \quad (7)$$

with $C = (3/\pi^3)\zeta(3) = 0.116$ and $\zeta(x)$ the Riemann zeta function. For atomic-scale disorder, the symmetry index $\beta = 1$ (orthogonal symmetry) and the degeneracy factor $s = 2$ (only spin degeneracy). For smooth disorder, one has $\beta = 4$ (symplectic symmetry) and $s = 4$ (both spin and valley degeneracy). In each case, the variance thus has the same value $\text{Var } G_{\text{UCF}} = C (W/L)(2e^2/h)^2$.

In Figs. 2b,3b we see that the conductance fluctuations approach the UCF value for sufficiently strong disorder. This is by itself remarkable, since the Altshuler-Lee-Stone theory requires *weak disorder*, such that the conductivity $\sigma \equiv \langle G \rangle L/W \gg e^2/h$. Our numerical data for $\text{Var } G$ only approaches $\text{Var } G_{\text{UCF}}$ when the disorder is so strong that $\sigma \simeq e^2/h$. For weaker disorder, the conductance fluctuations first rise to a peak value $\text{Var } G_{\text{peak}}$ well above $\text{Var } G_{\text{UCF}}$, and then drop to zero upon entering the ballistic regime.

The increase of the conductance fluctuations above the UCF value does not happen for the Anderson model of atomic-scale disorder (solid curves). For smooth disorder

the enhancement factor $\text{Var } G_{\text{peak}}/\text{Var } G_{\text{UCF}}$ increases with increasing Fermi energy μ_0 — it is therefore not restricted to the vicinity of the Dirac point. The enhancement factor also increases with increasing ξ (not shown), but at fixed ξ it is insensitive to the system size (compare open and filled symbols in Figs. 2b,3b). The anomalous enhancement does not, therefore, appear to be a finite-size effect. The transport mean free path (6) at $\mu_0 = \tau/2$ is $l_{\text{tr}} = 4\sqrt{3}a/K_0$ (for smooth disorder), so $l_{\text{tr}}/L \approx 0.1$ at the peak of maximal conductance fluctuations in the largest system considered. We would therefore expect to be well into the diffusive regime, but the UCF value characteristic of diffusion is not reached until the mean free path has been reduced by another factor of ten.

While the disappearance of the anomaly for atomic-scale disorder unambiguously indicates that the symplectic symmetry of the Dirac Hamiltonian is responsible for it, we have not been able to explain our simulations consistently in terms of existing transport theories for Dirac fermions [18, 19, 20, 21, 22, 23, 24, 25, 26]. Certain features of the data suggest a partial explanation.

First of all, at the Dirac point ($\mu_0 = 0$), the enhancement of the conductance fluctuations happens in the same range of disorder strengths as the enhancement of the conductivity above the ballistic value [16, 17]

$$\sigma_{\text{ballistic}} = \frac{4}{\pi} \frac{e^2}{h}. \quad (8)$$

This increase of σ was predicted by Titov [26] as a manifestation of resonant transmission of evanescent modes. We would expect such transmission resonances to enhance the mesoscopic fluctuations, but we would also expect the effect to diminish as the evanescent modes become propagating away from the Dirac point. Instead, the peak in $\text{Var } G$ becomes larger with increasing μ_0 , while the peak in σ disappears.

A second striking feature of the numerical data is that an increase of the impurity density $N_{\text{imp}}/N_{\text{tot}}$ and a decrease of the impurity potential δ at fixed K_0 has no significant effect on the conductance (compare the different open symbols in Figs. 2,3, which all lie approximately on a single curve). This signifies that the transition from the anomalously large fluctuations at weak disorder to the UCF value at stronger disorder is not related to the Born-Unitarity transition of Ref. [23] (which should appear at smaller K_0 for smaller $N_{\text{imp}}/N_{\text{tot}}$).

The percolation transition of Ref. [24] is more likely to be at the origin of the strong increase of the conductance fluctuations away from the Dirac point (where $k_F \xi \gtrsim 1$). One would expect the presence or absence of a percolating trajectory to produce large sample-to-sample fluctuations in the conductance, which would increase both with increasing k_F and with increasing ξ — as observed in our simulations. This interpretation would imply that the conductance fluctuations result from variations in *trajectories* rather than fluctuations in *phase shifts*.

To support this interpretation we compare in Fig. 4 the variance $\text{Var } G$ of the sample-to-sample fluctuations

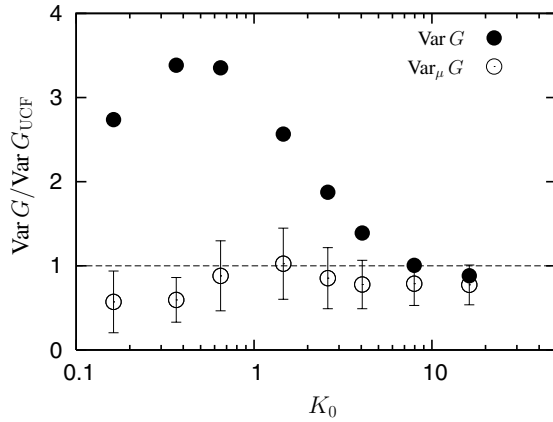


FIG. 4: Variance of the conductance away from the Dirac point ($\mu_0 = \tau/2$) as a function of disorder strength, for a square sample ($L = W = 121a$; $N_{\text{imp}}/N_{\text{tot}} = 0.045$). The filled symbols give the variance $\text{Var} G$ of the sample-to-sample fluctuations, while the open symbols give the variance $\text{Var}_\mu G$ of the energy-dependent fluctuations. (The latter quantity was calculated for a given sample by varying $\mu_0 \in (0.44\tau, 0.5\tau)$ and then averaging the resulting variance over 400 samples.)

with the variance $\text{Var}_\mu G$ of the fluctuations obtained in a given sample upon varying the Fermi energy μ_0 over a narrow interval. The former quantity contains contributions both from variations in trajectories and variations

in phase shifts, while in the latter quantity variations in phase shifts give the dominant contribution. To improve the numerical efficiency we took $W/L = 1$ for this comparison. The results for $\text{Var} G$ (filled symbols) are similar to those plotted in Fig. 3b for $W/L = 3.03$: A large enhancement appears of the sample-to-sample fluctuations above the UCF value. In contrast, the variance $\text{Var}_\mu G$ of the energy-dependent fluctuations (open symbols) does *not* show this enhancement, instead agreeing well with the UCF prediction [which for $W/L = 1$ equals $\text{Var} G_{\text{UCF}} = 0.186 \times (2e^2/h)^2$].

In the Altshuler-Lee-Stone theory of UCF one has $\text{Var} G = \text{Var}_\mu G$: Sample-to-sample fluctuations and fluctuations as a function of energy or magnetic field give the same variance. Our computer simulations imply that, remarkably enough, this so-called *ergodicity* of the mesoscopic fluctuations does not hold in graphene. An analytical theory to explain this unexpected numerical result is still lacking.

We thank J. H. Bardarson, V. I. Falko, G. Montambaux, and M. Titov for valuable discussions and correspondence. This research was supported by the Dutch Science Foundation NWO/FOM and by the European Community's Marie Curie Research Training Network (contract MRTN-CT-2003-504574, Fundamentals of Nanoelectronics). AR acknowledges support by the Polish Ministry of Science (Grant No. 1-P03B-001-29) and by the Polish Science Foundation (FNP).

-
- [1] B. L. Altshuler, JETP Lett. **41**, 648 (1985).
 - [2] P. A. Lee and A. D. Stone, Phys. Rev. Lett. **55**, 1622 (1985).
 - [3] C. W. J. Beenakker and H. van Houten, Solid State Phys. **44**, 1 (1991); cond-mat/0412664.
 - [4] E. Akkermans and G. Montambaux, *Mesoscopic Physics of Electrons and Photons* (Cambridge University, Cambridge, 2007).
 - [5] T. Ando, T. Nakanishi, and R. Saito, J. Phys. Soc. Japan **67**, 2857 (1998).
 - [6] N. H. Shon and T. Ando, J. Phys. Soc. Japan **67**, 2421 (1998).
 - [7] H. Suzuura and T. Ando, Phys. Rev. Lett. **89**, 266603 (2002).
 - [8] D. V. Khveshchenko, Phys. Rev. Lett. **97**, 036802 (2006).
 - [9] E. McCann, K. Kechedzhi, V. I. Fal'ko, H. Suzuura, T. Ando, and B. L. Altshuler, Phys. Rev. Lett. **97**, 146805 (2006).
 - [10] A. F. Morpurgo and F. Guinea, Phys. Rev. Lett. **97**, 196804 (2006).
 - [11] S. V. Morozov, K. S. Novoselov, M. I. Katsnelson, F. Schedin, L. A. Ponomarenko, D. Jiang, and A. K. Geim, Phys. Rev. Lett. **97**, 016801 (2006).
 - [12] X. Wu, X. Li, Z. Song, C. Berger, and W. A. de Heer, cond-mat/0611339.
 - [13] C. Berger, Z. Song, X. Li, X. Wu, N. Brown, C. Naud, D. Mayou, T. Li, J. Hass, A. N. Marchenkov, E. H. Conrad, P. N. First, and W. A. de Heer, Science **312**, 1191 (2006).
 - [14] H. B. Heersche, P. Jarillo-Herrero, J. B. Oostinga, L. M. K. Vandersypen, and A. F. Morpurgo, cond-mat/0612121.
 - [15] J. A. Vergés, F. Guinea, G. Chiappe, and E. Louis, cond-mat/0610201.
 - [16] M. I. Katsnelson, Eur. Phys. J. B **51**, 157 (2006).
 - [17] J. Tworzydło, B. Trauzettel, M. Titov, A. Rycerz, and C. W. J. Beenakker, Phys. Rev. Lett. **96**, 246802 (2006).
 - [18] N. M. R. Peres, F. Guinea, and A. H. Castro Neto, Phys. Rev. B **73**, 125411 (2006).
 - [19] V. V. Cheianov and V. I. Fal'ko, Phys. Rev. Lett. **97**, 226801 (2006).
 - [20] K. Ziegler, Phys. Rev. Lett. **97**, 266802 (2006).
 - [21] K. Nomura and A. H. MacDonald, cond-mat/0606589.
 - [22] I. L. Aleiner and K. B. Efetov, Phys. Rev. Lett. **97**, 236801 (2006).
 - [23] P. M. Ostrovsky, I. V. Gornyi, and A. D. Mirlin, Phys. Rev. B **74**, 235443 (2006).
 - [24] E. H. Hwang, S. Adam, and S. Das Sarma, cond-mat/0610157.
 - [25] S. Ryu, C. Mudry, A. Furusaki, and A. W. W. Ludwig, cond-mat/0610598.
 - [26] M. Titov, cond-mat/0611029.